



HAL
open science

Design of a 500 kW partially superconducting flux modulation machine for aircraft propulsion

Rémi Dorget, Sabrina Ayat, Rémy Biaujaud, Julien Tanchon, Jérôme Lacapere, Thierry Lubin, Jean Lévêque

► **To cite this version:**

Rémi Dorget, Sabrina Ayat, Rémy Biaujaud, Julien Tanchon, Jérôme Lacapere, et al.. Design of a 500 kW partially superconducting flux modulation machine for aircraft propulsion. *Journal of Physics: Conference Series*, 2021, 1975 (1), pp.012033. 10.1088/1742-6596/1975/1/012033 . hal-03445460

HAL Id: hal-03445460

<https://hal.science/hal-03445460>

Submitted on 24 Nov 2021

HAL is a multi-disciplinary open access archive for the deposit and dissemination of scientific research documents, whether they are published or not. The documents may come from teaching and research institutions in France or abroad, or from public or private research centers.

L'archive ouverte pluridisciplinaire **HAL**, est destinée au dépôt et à la diffusion de documents scientifiques de niveau recherche, publiés ou non, émanant des établissements d'enseignement et de recherche français ou étrangers, des laboratoires publics ou privés.



Distributed under a Creative Commons Attribution 4.0 International License

PAPER • OPEN ACCESS

Design of a 500 kW partially superconducting flux modulation machine for aircraft propulsion

To cite this article: R Dorget *et al* 2021 *J. Phys.: Conf. Ser.* **1975** 012033

View the [article online](#) for updates and enhancements.

You may also like

- [Development of Decision Support System for Solving the Machine Selection Problem in an Intermittent Manufacturing System Design](#)
P Buathong and A Vilasdaechanont
- [Development of Mirco-Machine Moving with Glucose and Hydrogen Peroxide](#)
Keitaro Yamazaki, Shingo Kaneko, Toyokazu Tanabe et al.
- [26th IAHR Symposium on Hydraulic Machinery and Systems](#)
Yulin Wu, Zhengwei Wang, Shuhong Liu et al.



The Electrochemical Society
Advancing solid state & electrochemical science & technology

241st ECS Meeting

May 29 – June 2, 2022 Vancouver • BC • Canada

Abstract submission deadline: Dec 3, 2021

Connect. Engage. Champion. Empower. Accelerate.
We move science forward



Submit your abstract



Design of a 500 kW partially superconducting flux modulation machine for aircraft propulsion

R Dorget^{1,2,*}, S Ayat¹, R Biaujaud¹, J Tanchon³, J Lacapere³, T Lubin²,
J Lévêque²

¹Safran Tech, Electrical & Electronic Systems Research group, Rue des Jeunes Bois, Châteaufort, 78114 Magny-Les-Hameaux, France

²Université de Lorraine, GREEN, F-54000 Nancy, France

³Absolut System, 2 Rue des Murailles, 38170 Seyssinet-Pariset, France

*remi.dorget@safrangroup.com

Abstract. Electric propulsion is seen as a potential solution for reducing greenhouse gas emissions from the aircraft industry. However, electrical machines must achieve high power to mass ratios (PtM) to meet aviation requirements. Superconducting technologies are a promising option for creating compact and efficient machines. Indeed, superconductors make it possible to generate large magnetic fields while reducing the need for ferromagnetic materials. In previous works, a 50 kW partially superconducting flux modulation machine has been realised. The flux modulation machine is an unconventional topology where the inductor is composed by a large static superconducting coil and rotating superconducting bulks acting as magnetic field shields. This topology allows controlling the inductor excitation while being brushless. In this paper, we design a 500 kW flux modulation machine considering the results of the 50 kW prototype and the constraints due to the structure change of scale. The presented machine aims to reach a power-to-mass ratio of 10 kW/kg.

1. Introduction

Meeting ambitious greenhouse gas emission reduction goals of the aviation industry requires innovative architectures such as turbo-electric or hybrid-electric propulsion [1,2]. These configurations require components with high power-to-mass ratios (PtM), for projects with a long-term timetable, electrical machines with a specific power higher than 10 kW/kg are required [3]. To achieve such PtM, high temperature superconductivity (HTS) technology is a promising solution by allowing high current densities and the generation of large magnetic fields. Indeed, technologies such as HTS machines or cables are considered for the realization of high performances propulsion systems [4]. Several studies have been carried out in the literature on HTS machines for aeronautics showing a great potential for mass reduction [5–12].

In this context, we are studying a partially superconducting flux modulation machine. As illustrated on figure 1, the flux modulation topology is composed by three main elements. The first part is a HTS coil fed by DC current which generate a magnetic field inside the machine. The second element is the machine rotor composed by several HTS bulks (one per pole pair). The last element comprises two three-phase armature which are made by arranging copper windings on both sides of the rotor. Thus, the studied flux modulation machine does not require any ferromagnetic parts. The HTS coil and the copper armatures are static components while the HTS bulks are the only rotary parts.



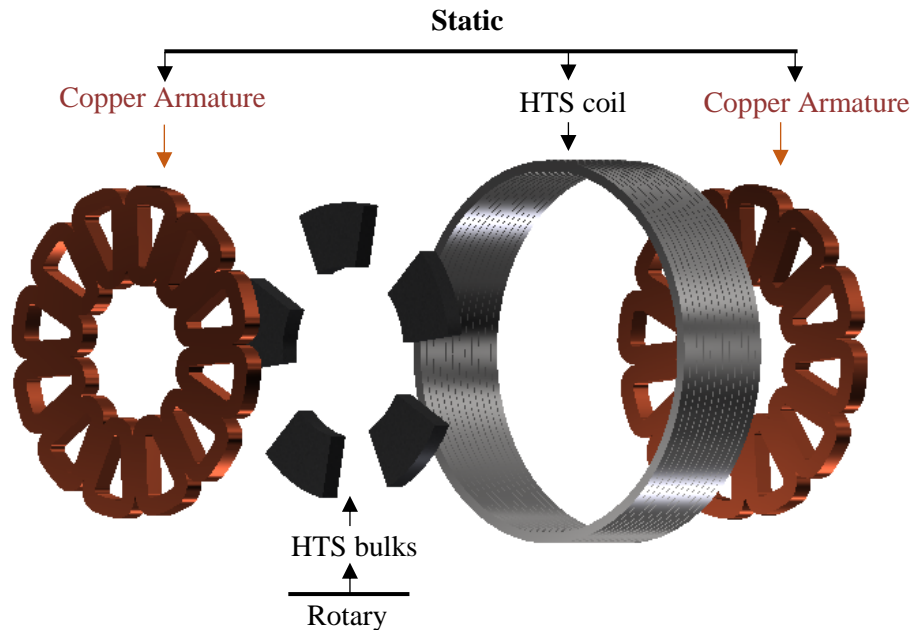


Figure 1. View of the flux modulation topology main elements.

The principle of operation of a flux modulation machine consists in using the HTS bulk diamagnetic behaviour to concentrate the axial flux created by the coil in the openings separating the bulks. To do so, the bulk operates at 30 K in the mixed state, the diamagnetic behaviour comes from the ability of the bulk to oppose the variation of magnetic field. The resulting flux density distribution in the air gap over a pole pair is shown in figure 2. On the bulk location the magnetic flux density is almost null while being increased elsewhere. Consequently, the resulting magnetic flux density shows a spatial variation in the air gap which will generate an electromotive force (EMF) in the three-phase armature when the bulks rotate. Thus, the flux modulation machine can be classified as an AC synchronous brushless topology. An interesting feature of this machine is to be able to control the magnetic loading through the coil without the need for slip rings contrary to conventional wound rotor machines.

A 50 kW prototype has been studied and realized in previous works (RESUM project) proving the feasibility of the technology [13,14]. In this article, we design a 500 kW flux modulation machine for its forthcoming construction in the project FROST (Flux-modulation ROTating Superconducting Topology). The aim of this design is to go from 50 kW to 500 kW without increasing the size or mass compared to the first prototype. The presented design takes into account the feedback of the first machine as well as the constraints due to the change of scale. The first part of this article lists the technical changes made to the various elements of the machine allowing for the envisaged power increase. A second part describes the modelling and sizing method for the machine. Finally, the electromagnetic design results are presented as well as the selected design for FROST.

2. Technological changes

2.1. HTS bulks

The rotor of the first prototype was composed by multi-seeded Y-Ba-Cu-O discs, each made from 4 seeds. Although multi-seeding allows large bulks to grow, it has been shown in the literature as well as in the first machine tests that these bulks have problems with grain-boundary homogeneity [15]. These grain-boundaries have a significant impact on the flux modulation and therefore on the machine performances [13]. In order to solve these issues in the FROST machine, single seeded Gd-Ba-Cu-O bulks have been selected. Furthermore, as shown in figure 3, the bulk shape is also changed, the previous

bulks were discs while those of FROST will be ring segments. This shape is more adapted to the machine structure.

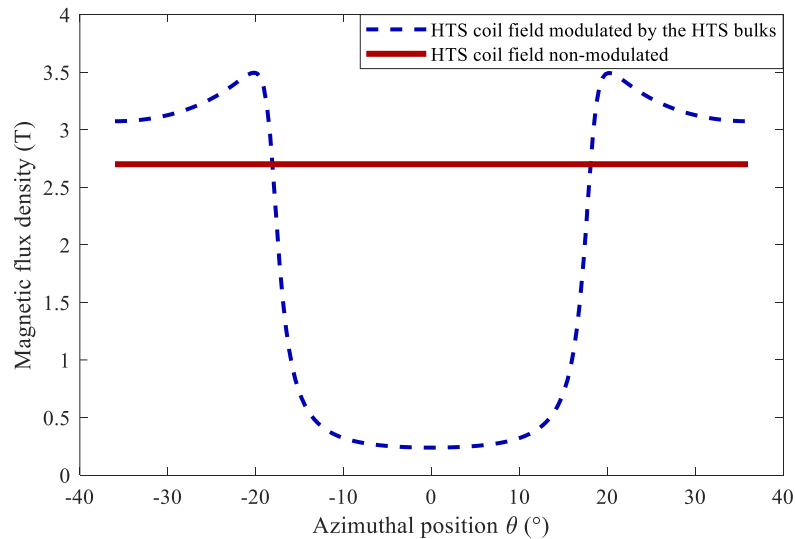


Figure 2. Air gap magnetic flux density modulated by the bulks over a pole pair.

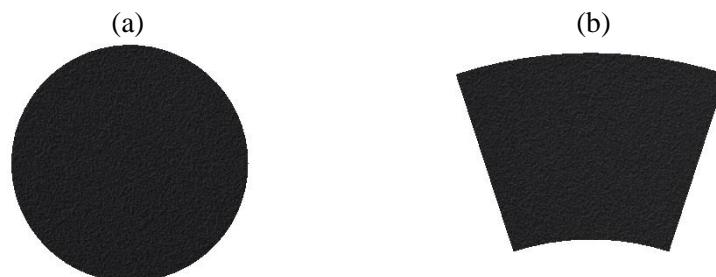


Figure 3. Shape of the superconducting bulks. (a) Y-Ba-Cu-O discs of the 50 kW RESUM machine. (b) Gd-Ba-Cu-O ring segments of the 500 kW FROST machine.

2.2. HTS coil

The second generation of HTS tapes can carry approximately three times the current density of the first generation while having a better flux pinning [16]. Thus, the magnetic field generated by a coil of the same size can be greatly increased by switching from 1G HTS tapes to 2G HTS tapes. The 50 kW prototype was built using a coil with 1G HTS tapes (Sumitomo new type HDI-BSSCO®). By switching to 2G HTS tapes, we can increase the magnetic loading of the topology by about a factor 3. However, particular attention must be paid to the mechanical resistance of this coil. Indeed, mechanical hoop stress estimated by the formula JBR [18] shows that switching from 1G to 2G can increase by a factor 9 the coil hoop stress. At last, the metal-as-insulation technique was chosen in order to increase the reliability in case of quench [17–19].

2.3. Copper armature

As a mean of reaching the required power, an improvement of the machine electrical loading is required. To achieve this, it has been decided here to increase the current density of the winding from 10 A/mm²

to 30 A/mm². Nevertheless, the armature cooling system must be adapted to be able to evacuate the large amount of generated heat in a compact volume.

The RESUM machine comprised a direct liquid cooling system, where a coolant is circulated directly on the armature windings. Two main axes are currently evaluated to increase the system heat extraction capability. Firstly, the RESUM machine made use of a thin back iron to guide the magnetic flux density. The increased magnetic flux density in the FROST machine would lead to the saturation of ferromagnetic materials, hence a back iron is no longer profitable. The removal of the back iron will improve the armature cooling, as the coolant will be in direct contact with the winding. Secondly, the diameter of the Litz wire strands in the windings will be reduced. Indeed, due to the absence of magnetic circuit, the armature windings are highly exposed to the varying magnetic field of the rotor. This would result in the generation of significant eddy-current loss components, if the strands section was not adapted. The estimation of the conductor losses are discussed in details later in this paper.

3. Machine sizing method

3.1. Overview and first parameters estimation

In order to design the machine properly, a number of geometrical parameters must be determined by an electromagnetic sizing. The main parameters to evaluate are the number of pole pairs, the external radius of the rotor, the winding cross section, the Litz wire strand diameter and the HTS coil dimensions. Some of these parameters are imposed by the technical choices made on the machine structure as well as supply constraints.

Firstly, the number of pole pairs is imposed by the winding layout and the machine operating frequency. In order to limit the eddy-current losses in the armature, the machine operating frequency has to be as low as possible. As the machine rotating speed is fixed, this means that the number of pole pairs should be limited. A concentrated winding has been selected to reduce the size of the armature end-windings. Building a concentrated winding without EMF harmonics of even order, thus having low torque oscillations, is only possible for certain number of pole pairs [20]. Here, the smallest compatible number of pole pairs was 5, which lead to a machine operating frequency of 400 Hz. Secondly, the rotor diameter is imposed by the maximum size of ring segment shaped bulks available. The bulks shown above allow the design of a rotor with an external radius of 148 mm and a bulk internal radius of 85 mm.

3.2. Torque calculation

Now that the rotor dimensions are fixed, the electromagnetic sizing must determine the dimensions of the HTS coil as well as the copper armature. The maximum torque of an axial flux machine T_{em} can be expressed by:

$$T_{em} = 3pK_w\Phi NI \quad (1)$$

Where p is the number of pole pairs, Φ is the RMS value of the fundamental magnetic flux under a pole, NI is the Ampere-turns per phase of the armature and K_w is the winding coefficient. The winding coefficient K_w can be calculated analytically for an iron-less armature as described in [21]. NI can be obtained from:

$$NI = 8K_fJS_w \quad (2)$$

Where J is the RMS current density in the stator fixed above at 30 A/mm², S_w the winding cross section and K_f the winding filling factor. Ultimately, assuming a very compacted Litz wire, we can calculate the theoretical maximum value of K_f with the following equation:

$$K_f = \frac{\pi}{2\sqrt{3}} \frac{d_s^2}{(d_s + e_i)^2} \quad (3)$$

Where d_s is the Litz strand diameter and e_i the strand insulation thickness. Equation (3) shows that the theoretical filling factor decreases sharply when a very thin Litz wire strand diameter is chosen which

has an impact on the torque though it reduces the Eddy-current losses. Since the filling factor of a Litz wire never reaches the theoretical maximum value, one can use the trend obtained by this equation and calculate a value closer to reality by assuming that the real factor is 90% of the theoretical factor for a compact wire.

Lastly, Φ is related to the magnetic flux density generated by the coil and modulated by the bulks. This value is computed numerically by modelling the HTS coil and bulks in a 3D model on COMSOL Multiphysics. The inductor model is a stationary A-formulation where 1/4 of a pole pair is simulated according to the symmetries. The bulk is defined as a magnetic region with a relative permeability of 10^{-4} while the coil is modelled as a uniform current density.

3.3. Losses calculation

The copper armature is subjected to two major kind of losses, conduction losses and Eddy-current losses. The conduction losses per unit of length p_c of a strand can be obtained from:

$$p_c = \rho J^2 \frac{\pi}{4} \quad (4)$$

Where ρ is the copper resistivity. Due to the absence of a magnetic circuit, eddy current losses p_e are greater than in conventional machines and must therefore be calculated precisely. For a single strand subjected to a sinusoidal magnetic field of amplitude B_{max} and pulsation ω , the eddy current losses can be calculated from:

$$p_e = \frac{\pi \omega^2 d_s^4 B_{max}^2}{128\rho} \quad (5)$$

The equations (4) and (5) are obtained by neglecting the skin effect, more complex formulas considering it involving kelvin functions can be found in [22,23]. However, for frequencies below 10 kHz, equations (4) and (5) are precise enough and it is not necessary to take into account the skin effect. In the case of our machine, the frequency of the fundamental being about 400 Hz, even the harmonics are not impacted and their contribution can be calculated from (4) and (5).

As the magnetic field created by the armature is an order of magnitude smaller than the inductor one, the eddy current associated with the armature own excitation can be neglected. To calculate the latter, one must consider the distribution of the inductor magnetic field throughout the armature as well as all its harmonics and calculate the losses strand by strand. For this purpose, we use the method presented and tested in [24].

4. Results

On the basis of the previous method, a study was carried out to determine the armature and HTS coil to maximise the machine PtM. Here various configurations are being compared, for each of them the dimensions of the coil are fixed while the winding cross section is determined to reach the desired power.

In figure 4, the PtM of several 500 kW design are shown, with regards to the magnetic field generated by the coil, this value is related to the dimensions of the coil and therefore to Φ in equation (1). The masses of the motor include the active masses as well as the non-active mechanical masses calculated from an extrapolation on the basis of those of RESUM. This graph clearly shows the existence of an optimum between the armature and the HTS coil. Indeed, a decrease in the critical current density of HTS tapes with the applied magnetic field means that their mass efficiency decreases with their size. Likewise, the absence of a magnetic circuit means that the field in the armature is inhomogeneous, the turns of the copper windings furthest away from the air gap see a lower flux than the turns at the front. Thus, for both the armature and the HTS coil, each new turn is less efficient than the previous one, so the electromagnetic design mainly consists in finding the balance between these two phenomena.

As shown in figure 5, the losses are greater for machines with large armature Ampere-turns NI which implies that the majority of losses are conduction losses. Eddy current losses still account for a non-negligible part of the losses, but the use of a Litz wire with 0.2 mm in diameter strands greatly reduces their impact on the efficiency.

At last, table 1 presents the performances of the design selected for the FROST project as well as those of the RESUM prototype. According to our results, the technological choices and improvements planned on the topology make it possible to reach 500 kW while keeping a machine of the same size and mass. The latter should even be slightly reduced by the removal of the back-iron. Eventually, the machine should be able to reach 10 kW/kg.

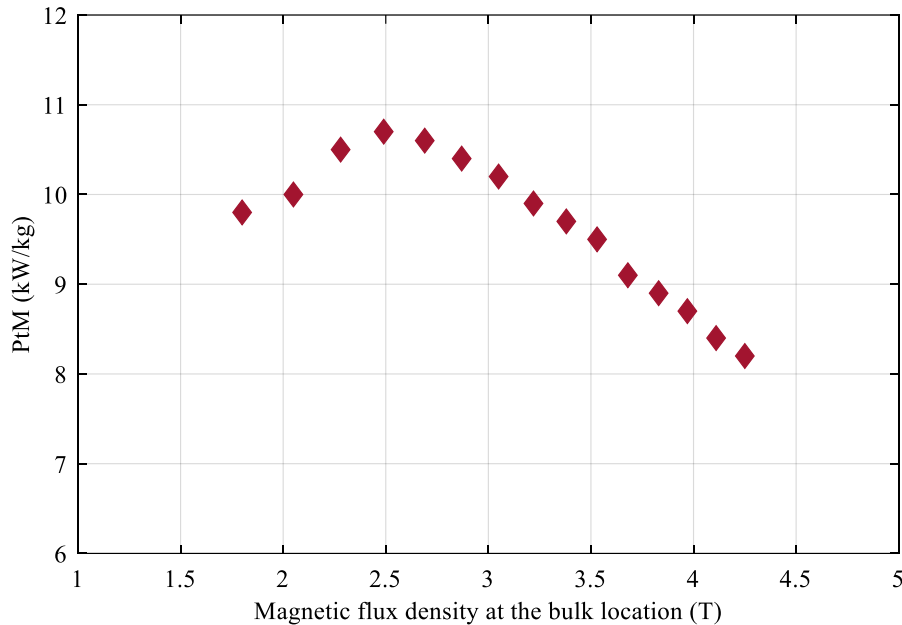


Figure 4. Power-to-mass ratios of several 500 kW designs versus the magnetic flux density generated by the coil.

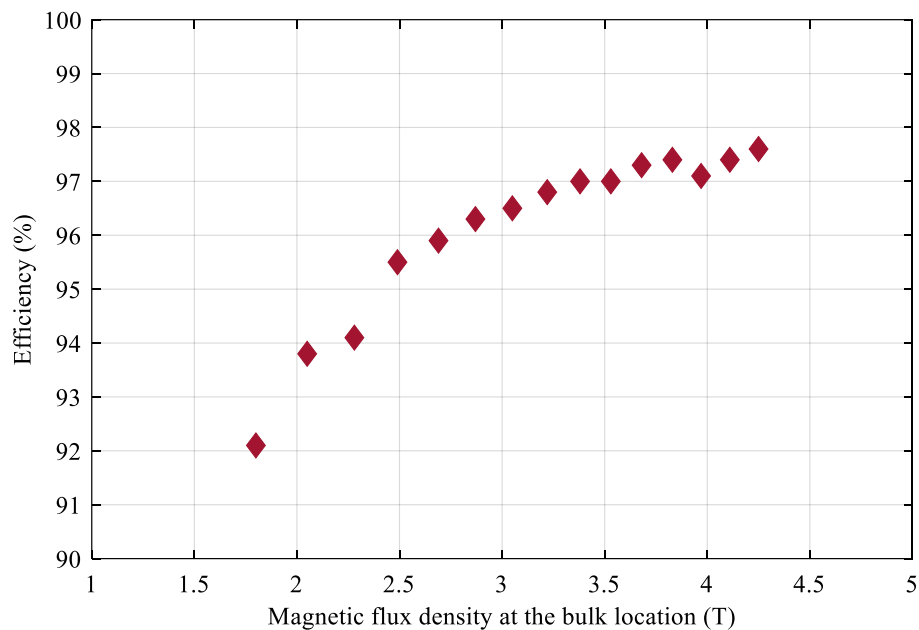


Figure 5. Efficiency of several 500 kW designs versus the magnetic flux density generated by the coil.

Table 1. Comparison of FROST's expected performances relative to RESUM.

Type	RESUM [13]	FROST
Designed power	50 kW	500 kW
Rated rotating speed	5000 rpm	5000 rpm
Pole pairs	5	5
Rated armature voltage	230 V	230 V
Rated armature current	72 A	725 A
Operating HTS temperature	30 K	30 K
Total mass	52 kg	50.2 kg
Conduction losses	1.2 kW	22.1 kW
Eddy-current losses	1.8 kW	2.2 kW

5. Conclusion

The electromagnetic design of a 500 kW machine has been presented. The design has been informed from numerical and experimental data from a 50 kW prototype based on the same topology. By introducing changes to the HTS tape technology used, the bulks and the current density in the armature, we intend to achieve the desired power while keeping certain parameters such as the rotating speed, the HTS operating temperature and the machine mass unchanged. Hence, we expect to reach 10 kW/kg during the course of this project.

The construction and testing of the machine will have to confirm these results. Some technical issues need to be resolved in order to achieve the realisation of this machine. A rotating vacuum sealing resistant to magnetic fields must be found and the ability of the bulks to modulate the field homogeneously must be proven experimentally. We also plan to work on reducing the machine's inactive masses (cryostat, shaft, etc) to further improve the power-to-weight ratio, since they currently account for half of the machine's total weight.

Acknowledgments

The authors would like to thank the Direction Générale de l'Armement (DGA), the Agence de l'Innovation de Défense (AID) and the Agence Nationale de la Recherche (ANR), project "ANR-19-ASMA-0001", for the support and funding of this work.

References

- [1] Jansen R, Brown G V, Felder J L and Duffy K P Turboelectric Aircraft Drive Key Performance Parameters and Functional Requirements *51st AIAA/SAE/ASEE Joint Propulsion Conference* (American Institute of Aeronautics and Astronautics)
- [2] Kim H D, Perry A T and Ansell P J 2018 A Review of Distributed Electric Propulsion Concepts for Air Vehicle Technology *2018 AIAA/IEEE Electric Aircraft Technologies Symposium (EATS) 2018 AIAA/IEEE Electric Aircraft Technologies Symposium (EATS)* pp 1–21
- [3] Medicine N A of S Engineering, and, Sciences D on E and P, Board A and S E and Emissions C on P and E S to R C A C 2016 *Commercial Aircraft Propulsion and Energy Systems Research: Reducing Global Carbon Emissions* (National Academies Press)
- [4] Boll M, Corduan M, Biser S, Filipenko M, Pham Q H, Schlachter S, Rostek P and Noe M 2020 A holistic system approach for short range passenger aircraft with cryogenic propulsion system *Supercond. Sci. Technol.* **33** 044014
- [5] Masson P J, Breschi M, Tixador P and Luongo C A 2007 Design of HTS Axial Flux Motor for Aircraft Propulsion *IEEE Transactions on Applied Superconductivity* **17** 1533–6
- [6] Masson P J and Luongo C A 2005 High power density superconducting motor for all-electric aircraft propulsion *IEEE Transactions on Applied Superconductivity* **15** 2226–9

- [7] Haran K S, Kalsi S, Arndt T, Karmaker H, Badcock R, Buckley B, Haugan T, Izumi M, Loder D, Bray J W, Masson P and Stautner E W 2017 High power density superconducting rotating machines—development status and technology roadmap *Supercond. Sci. Technol.* **30** 123002
- [8] Berg F, Palmer J, Miller P, Husband M and Dodds G 2015 HTS Electrical System for a Distributed Propulsion Aircraft *IEEE Transactions on Applied Superconductivity* **25** 1–5
- [9] Masson P J and Luongo C A 2007 HTS Machines for Applications in All-Electric Aircraft 2007 *IEEE Power Engineering Society General Meeting 2007* IEEE Power Engineering Society General Meeting pp 1–6
- [10] Luongo C A, Masson P J, Nam T, Mavris D, Kim H D, Brown G V, Waters M and Hall D 2009 Next Generation More-Electric Aircraft: A Potential Application for HTS Superconductors *IEEE Transactions on Applied Superconductivity* **19** 1055–68
- [11] Terao Y, Kong W, Ohsaki H, Oyori H and Morioka N 2018 Electromagnetic Design of Superconducting Synchronous Motors for Electric Aircraft Propulsion *IEEE Transactions on Applied Superconductivity* **28** 1–5
- [12] Filipenko M, Kühn L, Gleixner T, Thummet M, Lessmann M, Möller D, Böhm M, Schröter A, Häse K, Grundmann J, Wilke M, Frank M, Hasselt P van, Richter J, Herranz-Garcia M, Weidemann C, Spangolo A and Klöpzig M 2020 Concept design of a high power superconducting generator for future hybrid-electric aircraft *Supercond. Sci. Technol.* **33** 054002
- [13] Colle A, Lubin T, Ayat S, Gosselin O and Leveque J 2020 Test of a Flux Modulation Superconducting Machine for Aircraft *J. Phys.: Conf. Ser.* **1590** 012052
- [14] Colle A, Lubin T, Ayat S, Gosselin O and Lévêque J 2019 Analytical Model for the Magnetic Field Distribution in a Flux Modulation Superconducting Machine *IEEE Transactions on Magnetics* **55** 1–9
- [15] Werfel F N, Floegel-Delor U, Riedel T, Goebel B, Rothfeld R, Schirrmeister P and Wippich D 2013 Large-scale HTS bulks for magnetic application *Physica C: Superconductivity* **484** 6–11
- [16] Wimbush S C and Strickland N M 2017 A Public Database of High-Temperature Superconductor Critical Current Data *IEEE Transactions on Applied Superconductivity* **27** 1–5
- [17] Lécresse T and Iwasa Y 2016 A (RE)BCO Pancake Winding With Metal-as-Insulation *IEEE Transactions on Applied Superconductivity* **26** 1–5
- [18] Fazilleau P, Borgnic B, Chaud X, Debray F, Lécresse T and Song J-B 2018 Metal-as-insulation sub-scale prototype tests under a high background magnetic field *Supercond. Sci. Technol.* **31** 095003
- [19] Lécresse T, Badel A, Benkel T, Chaud X, Fazilleau P and Tixador P 2018 Metal-as-insulation variant of no-insulation HTS winding technique: pancake tests under high background magnetic field and high current at 4.2 K *Supercond. Sci. Technol.* **31** 055008
- [20] Bianchi N and Pré M D 2006 Use of the star of slots in designing fractional-slot single-layer synchronous motors *IEE Proceedings - Electric Power Applications* **153** 459–66
- [21] Kamper M J, Wang R-J and Rossouw F G 2008 Analysis and Performance of Axial Flux Permanent-Magnet Machine With Air-Cored Nonoverlapping Concentrated Stator Windings *IEEE Transactions on Industry Applications* **44** 1495–504
- [22] Lammeraner J and Štafl M 1966 *Eddy Currents* (CRC Press)
- [23] Tourkhani F and Viarouge P 2001 Accurate analytical model of winding losses in round Litz wire windings *IEEE Transactions on Magnetics* **37** 538–43
- [24] Rong-Jie Wang and Kamper M J 2004 Calculation of eddy current loss in axial field permanent-magnet machine with coreless stator *IEEE Transactions on Energy Conversion* **19** 532–8